

Article

Experimental and Numerical Investigation on Structural Performance of Steel Deck Plate Bolted with Truss Girder

Jinwon Shin ¹ , Jineung Lee ², Yongjae Lee ³ and Byungyun Kim ^{1,*}¹ Department of Architectural Engineering, Catholic Kwandong University, Gangneung 25601, Korea² Hyosung Corporation, Mapo-gu, Seoul 04144, Korea³ Department of Architecture, Dongyang Mirae University, Seoul 08221, Korea

* Correspondence: kby@cku.ac.kr; Tel.: +82-33-649-7528

Received: 18 July 2019; Accepted: 1 August 2019; Published: 4 August 2019



Abstract: This paper presents an experimental and numerical study to investigate the structural performance of a steel deck-plate system bolted with truss girder. This system has been proposed herein to resolve the issues caused by welding. Structural tests for six full-scale specimens were performed to ensure the structural safety of the proposed system based on design criteria for deflection. Local responses with an emphasis on the failure modes of the system were also assessed using the measured strains at the locations where stresses are localized. Numerical models for all test specimens were developed with the material test data and were validated based on the test results. The structural behaviors of the proposed system, not confirmed in the tests, were further examined using numerical simulations, with a focus on the failure mechanism between the numerical predictions and the test results.

Keywords: steel deck plate bolted with truss girder; structural safety; experimental evaluation; numerical validation; stress localization

1. Introduction

Floor systems using deck plates have been often used in construction sites, especially for high-rise buildings. A wide variety of deck-plate structural and manufacturing systems have been developed by many research institutions and construction companies due to their better structural performance and inherent construction efficiencies [1–4]. The deck plate serves as a form for concrete placement, thereby reducing the construction period and expense, noting that the concrete formwork generally occupies approximately thirty percent of the total construction cost [5]. Also, the deck-plate systems provide work space and the deck plate itself plays a role as a flexural member, which can resist the self-weight of concrete to pour and the workload during the construction period.

The deck-plate system integrated with truss girder by welding has been frequently used these days because of its structural performance suited to high-rise and long-span buildings [3,6]. The structural safety of this truss deck plate has been evaluated and verified by several researchers [5,7–11], and they are currently being used in a number of construction sites.

The validity for the structural performance of the truss girder-integrated (welded) deck plates have been demonstrated, as described previously, but the welded joints have caused problems such as the loss of zinc-coated section and the subsequent corrosion when used in wet and poorly ventilated areas, spoiling the beauty of the slab [12,13]. Moreover, it has been difficult to identify the cracks occurring inside the slab because the steel sheet cannot be detached after concrete hardening. Kim et al. [3] proposed a deck-plate system with non-welding truss-type deformed steel wires (TOX deck-plate

slab) to solve these sorts of problems. This system involved pressure joining in lieu of spot welding to connect lattice to galvanized steel sheets and does not require welding, thereby not suffering an oxidation-induced rust. For this non-welding deck-plate system, there is, however, still a limitation that the deck plate is hard to decouple from the slab, which makes checking the crack, if any, inside the slab and recycling the deck plate difficult.

This study thus proposes a deck plate, made of galvanized steel sheet, connected by bolts rather than welding to enable the deck plate to be reused, thereby preventing corrosion for the deck plate, facilitating grasping of the cracks of the slab, and developing an eco-friendly construction method for deck plate. Six full-scale tests were performed to investigate the structural performance of the proposed deck-plate system bolted with truss girder. Three slab depths of 135, 150, and 200 mm and the corresponding span lengths of 3200, 3800, and 4500 mm, respectively, were considered. Local failure modes were examined using measurements from plastic strain-gauges. A numerical study was then performed using a finite element code, LS-DYNA [14,15], to ensure that the observations from the tests were reliable and to further investigate the global and local responses, which were not confirmed during the tests. The numerically derived failure modes are discussed in detail by comparison to the test results.

2. Deck Plate Bolted with Truss Girder

The deck-plate systems bolted with triangular truss girder, as introduced previously, are produced automatically by the machine at the factory, such that this slab system is manufactured under well-organized quality control and can maintain a constant spacing of reinforcing bars with yielding high-quality products. Since the truss girder and the galvanized steel sheet are assembled by bolts, the steel sheet can be disassembled after the completion of the construction, by simply dismantling the bolts after the concrete pouring and curing are finished. Accordingly, this deck-plate system can be considered as an eco-friendly method that can recycle resources, compared to the existing truss girder-integrated deck plates.

The manufacturing process of this eco-friendly deck-plate system at the factory is divided largely into two processes. The first process involves fabrication of a triangular truss girder consisting of one upper rebar, two lower rebars, and lattice steel wires by welding, as shown in Figure 1. Secondly, deck plates are made by forming corrugations at appropriate intervals on galvanized steel sheets. When these two manufacturing processes are completed, the truss girder and the deck plate are assembled using spacers and bolts, as shown in Figure 2. Spacers are located on the deck plate with intervals of 400 mm. This truss girder-bolted deck plates are fabricated to have a width of 600 mm and a slab thicknesses from 120 mm to 300 mm, where it is possible to design a camber considering an expected deflection for a given construction load.

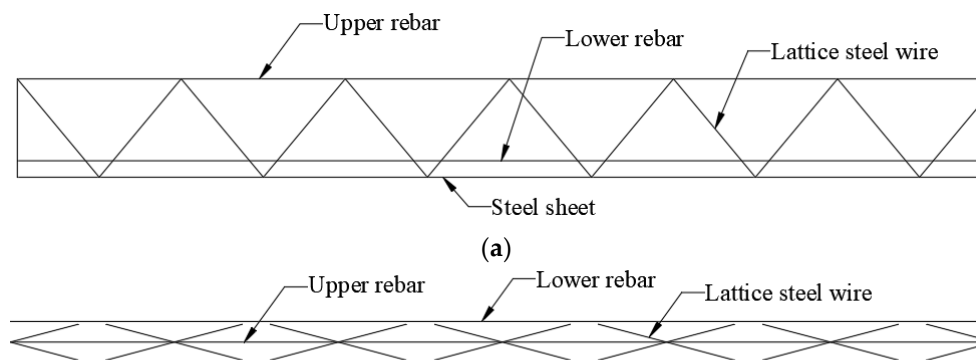


Figure 1. Deck-plate system bolted with truss girder. (a) Side view. (b) Top view.

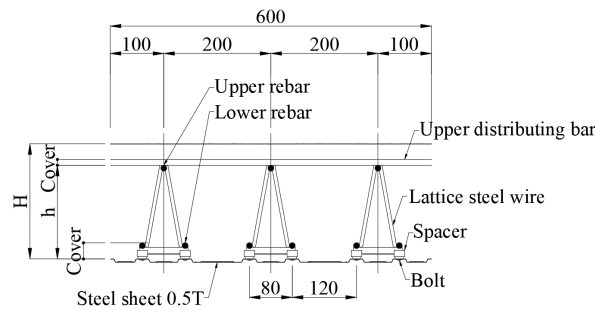


Figure 2. Section detail for the truss girder-bolted deck plate.

3. Test Preparation

3.1. Specimen Design

Total six full-scale specimens were prepared to evaluate the structural safety of the proposed truss girder-bolted deck plates, introduced previously, subjected to a specified construction load. The text matrix including the primary design parameters is presented in Table 1.

Table 1. Text matrix.

No	Specimen ID	Upper Rebar (mm)	Lower Rebar (mm)	Lattice Steel Wire (mm)	Depth (mm)	Span (mm)
1	135-ED1-3.2A	10	8	5	135	3200
2	135-ED1-3.2B	10	8	5	135	3200
3	150-ED3-3.8A	13	8	5	150	3800
4	150-ED3-3.8B	13	8	5	150	3800
5	200-ED5-4.5A	13	13	6	200	4500
6	200-ED5-4.5B	13	13	6	200	4500

Three types of specimens were considered, and two tests with the same specimen design were allocated for each type, i.e., Nos. 1 and 2, 3 and 4, and 5 and 6 were designed identically. Specimen ID was defined using the main design parameters of the test specimens, for example, the ID of specimen No. 1 of 135-ED1-3.2A indicates, in order, the entire slab depth of 135 mm, type 1 (ED1) associated with the member sizes of the truss girder comprising upper rebar, lower rebar, and lattice steel wire, the span length of 3200 mm, and the orders of test, A (the first) and B (the second). The actual truss girder-bolted deck-plate system used in the field has a width of 600 mm with three rows of truss girder, as shown in Figure 2, but the test specimens were designed with a width of 400 mm and two rows of truss girder due to the limited environmental conditions of the laboratory, as shown in Figure 3. The overall experimental view is shown in Figure 4.

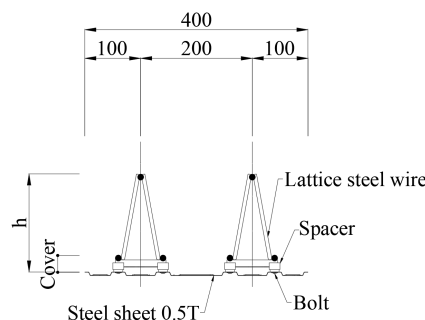


Figure 3. Section detail for test specimens of truss girder-bolted deck plates.



Figure 4. Experimental view.

3.2. Primary Design Parameter

The primary design parameters of the deck plate bolted with truss girder were slab depth, members of truss girder of upper rebar, lower rebar and lattice steel wires, and span length. The slab depth and the truss member varied with the relevant span length. Three slab depths of 135 mm, 150 mm, and 200 mm were determined according to the corresponding span lengths of 3200 mm, 3800 mm, and 4500 mm, respectively. Diameters of 5, 6, 8, 10, and 13 mm were used for the truss-girder components, noting that larger diameters were used for longer span length, as shown in Table 1. These test specimens are assessed using design criteria, as described in the following section.

3.3. Design Criteria

The structural performance of the proposed bolted deck plate has been evaluated using deflection criteria per AIK [16], which provides more conservative criteria than ASCE [17]. The allowable deflection limits were thus defined as the length of clear span divided by 210 mm. The capability to restore the deflection was examined by unloading when the maximum construction load, defined for each specimen, was reached. The failure mechanism of the proposed system was also investigated by applying loads until the specimens lastly fail.

3.4. Loading and Boundary Conditions

Test specimens were subjected to uniformly distributed construction loads calculated in consideration of self-weights of deck plate and non-hardened concrete and workload, as shown in Table 2. The self-weight of deck plate with a thickness of 0.5 mm was defined as 0.25 kN/m² for all specimens; those of non-hardened concrete are determined depending on their slab depths and were 3.1 kN/m², 3.45 kN/m², and 4.6 kN/m² for 135-ED1-3.2, 150-ED3-3.8, and 200-ED5-4.5, respectively. In addition to these dead loads, workloads involving construction machines, various materials, workers, and so on were assumed to be 1 kN/m² for all specimens. The total construction loads, therefore, became 4.35, 4.70, and 5.85 kN/m² for specimens, 135-ED1-3.2, 150-ED3-3.8, 200-ED5-4.5, respectively.

Table 2. Construction load.

Specimen Type	Clear Span (mm)	Construction Load (kN/m ²)			
		Self-Weight of Deck Plate	Self-Weight of Concrete	Workload	Total
135-ED1-3.2	3100	0.25	3.10	1	4.35
150-ED3-3.8	3700	0.25	3.45	1	4.70
200-ED5-4.5	4400	0.25	4.60	1	5.85

All three specimens were simply supported at 50 mm from both ends, indicating that the clear spans became 3100, 3700, and 4400 mm, respectively. The uniform loads were assigned to the deck plates using two kinds of loading plates of rectangular support and weight plates, as shown in Figure 5. Because these loading plates could not be simultaneously placed on the deck plates to realize the uniformly distributed loading conditions, they were assigned conservatively one by one from the center of the deck plate to the end. The weights of single support and weight plates were 80 and 40 N, respectively, which were measured prior to conducting the tests. The loading method is shown in Figure 6, which shows that the support plates are inserted between the lower re-bars and the deck plate, and the weight plates are attached to both sides of the support plates. The loading conditions for 135-ED1-3.2A is shown in Figure 7.

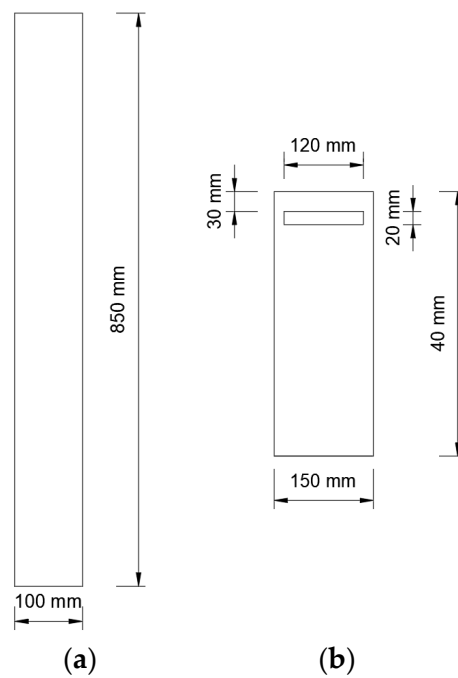


Figure 5. Loading equipment. (a) Support plate (80 N for each). (b) Loading plate (40 N for each).

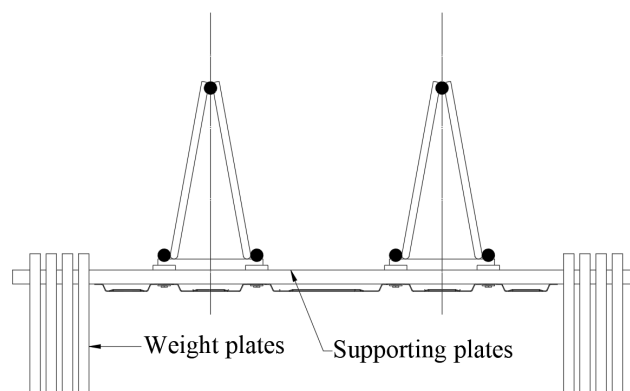


Figure 6. Loading method.

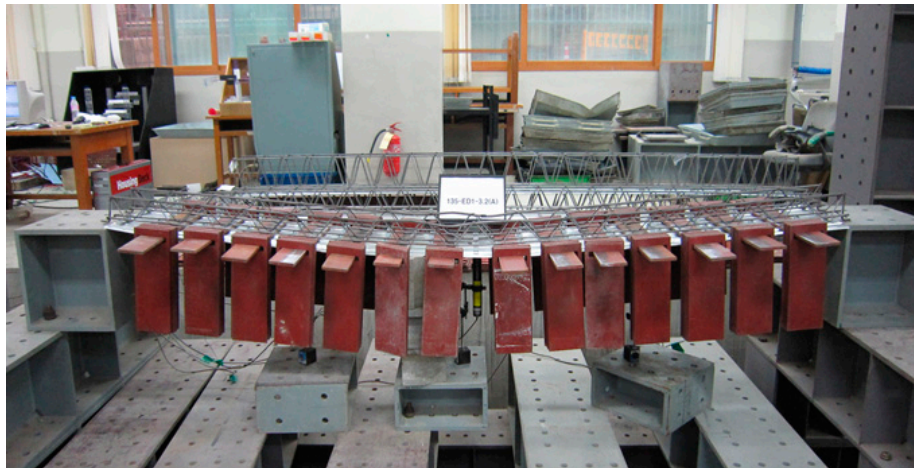


Figure 7. Loading conditions for 135-ED1-3.2.

The tests were performed in two steps. The specimens were loaded until the specified construction loads, provided in Table 2, were reached and were unloaded completely to evaluate the restoring capability, respectively. The loads were then applied to the maximum in order to observe the failure modes of the specimens. The overall test set-up is shown in Figure 8.

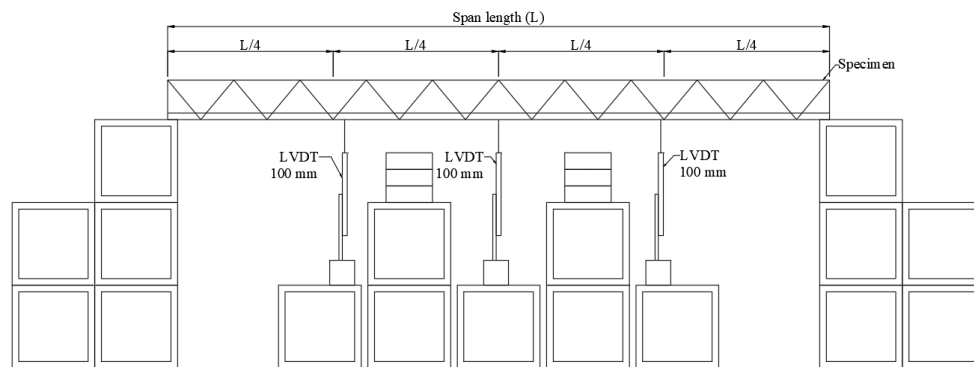


Figure 8. Test set-up.

3.5. Deflection and Strain Measuring Plan

The deflections of the specimens were measured using LVDT at three locations dividing the span length by four, as shown in Figure 8. Local responses of deck plate bolted with truss girder were evaluated using strain-gauges, as shown in Figure 9, which shows the strain-gauge locations. Five strain-gauges of S1, S2, L1, L2, and P1 were installed at the locations for which stresses are expected to be maximum, that is, S1 on the center of the upper rebar, S2 on the center of the lower rebar, and L1 and L2 on the mid-height of the diagonal lattice steel wires near both ends, and P1 on the center of the deck plate. Failure modes observed in the test results are discussed later in this paper using the strain-gauge measurements.

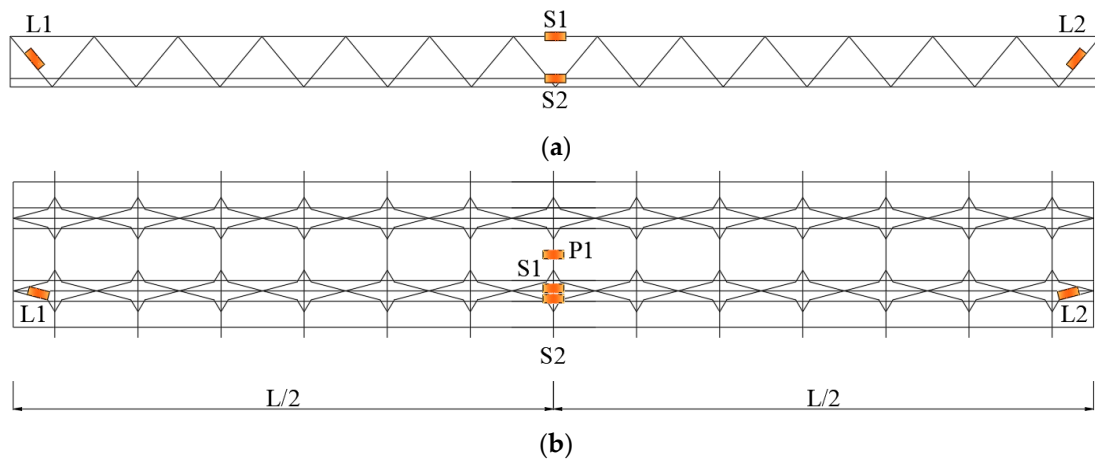


Figure 9. Strain-gauge plan. (a) Side view. (b) Top view.

4. Test Results

4.1. Material Tests

Tensile tests were performed to evaluate the mechanical properties of steel components used for test specimens, that is, the SWM-R steel with diameters of 8, 10, and 13 mm used for upper and lower rebars, the SWM-R steel with diameters of 5 and 6 mm used for lattice steel wires, and the SGC 570 steel with a thickness of 0.5 mm used for deck plate. Results are presented in Table 1, where mean values for three specimens for each material are used.

KATS [18] specifies the nominal tensile strength greater than 540 MPa for SWM-P and the nominal yield and tensile strengths greater than 440 MPa and 540 MPa, respectively, for SWM-R. It has been confirmed that the SWM-P and SWM-R steels satisfy the standard, as shown in Table 3. For SGC 560Y (SGC 570), KATS [19] specifies its yield and tensile strengths of 560 and 570, respectively, but the tensile tests somewhat underpredicted both the yield and tensile strengths. It was thus observed in the structural tests if this would affect the overall structural performance.

Table 3. Results of material tests.

Coupon	Diameter/Thickness (mm)	Steel Type	Yield Strength (MPa)	Yield Strain (10^{-6})	Tensile Strength (MPa)	Elongation (%)
Upper/Lower rebar	13	SWM-R	548	2330	693	12.8
Upper rebar	10	SWM-R	628	2700	713	12.0
Lower rebar	8	SWM-R	542	2680	582	13.3
Lattice steel wire	5	SWM-P	532	2560	582	22.7
	6	SWM-P	519	2560	624	17.8
Steel sheet	0.5	SGC 570	464	2320	546	24.3

Figure 10 shows stress–strain curves obtained from tensile tests for SWM-R with the 10 mm diameter and SGC 570 with the 0.5 mm diameter used for deck plate. Results for other steel materials are provided in detail in Lee [20]. The material test data given in Table 3 were used in the numerical simulations and the results are discussed based on the test results for the proposed truss girder-bolted deck plate.

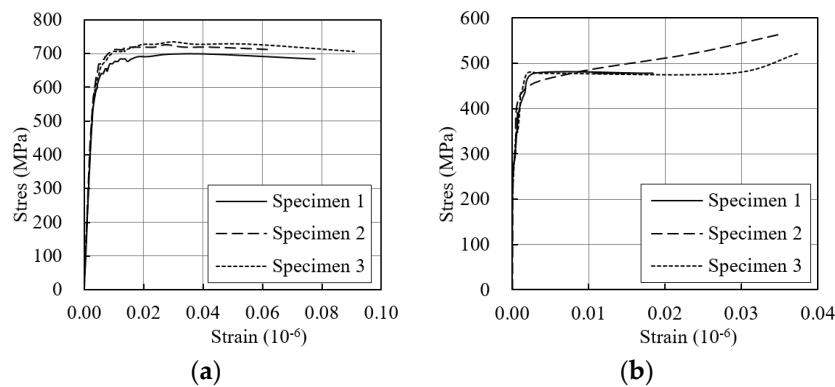


Figure 10. Stress–strain curves obtained from tensile tests. (a) SWM-R, 10 mm. (b) SGC 570.

4.2. Specimens 135-ED1-3.2A and B

Specimens 135-ED1-3.2A and B have the slab thickness of 135 mm and comprise the upper rebar with a diameter of 10 mm, the lower rebar with a diameter of 8 mm, the lattice steel wire with a diameter of 5.0 mm, and the deck plate with a thickness of 0.5 mm. The construction load used to evaluate the deflection was specified to be 4.35 kN/m², and the actual construction load in the test was measured as 4.38 kN/m², which was close to the specified construction load.

Figure 11 shows the distributed loads as a function of deflection measured at three locations for specimen, 135-ED1-3.2A and B. The maximum deflection at the center of the specimen for the specified construction load for 135-ED1-3.2A was measured as 20.5 mm, and the residual deflection was 0.57 mm with the restoration rate of 97.2% when unloaded, indicating that this specimen has the higher restoration capability, as expected. Similar observations were made for 135-ED1-3.2B: the maximum deflection at the center was 23.0 mm and the residual deflection at the unloading was 0.40 mm and 98.3%. For both specimens A and B, the left and right deflections were similar, indicating the load was not biased over the entire span.

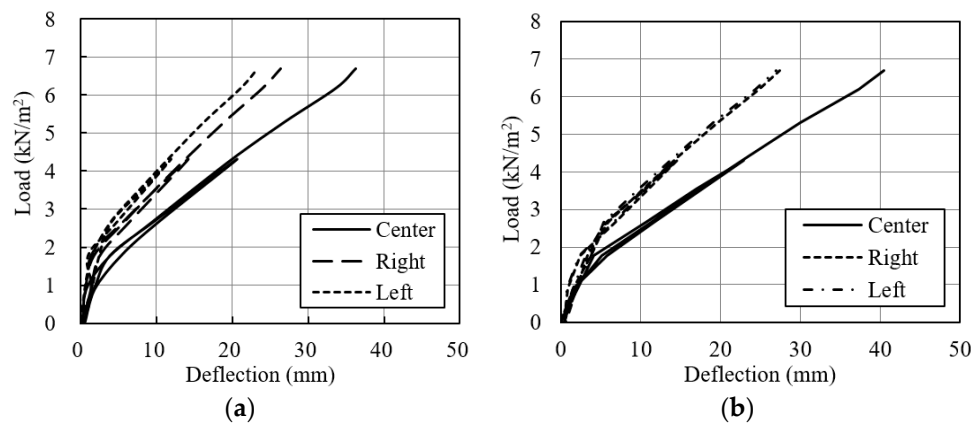


Figure 11. Distributed load as a function of deflection for (a) Specimen 135-ED1-3.2A and (b) Specimen 135-ED1-3.2B.

4.3. Specimens 150-ED3-3.8A and B

Specimens 150-ED3-3.8A and B have been designed to have the slab depth of 150 mm and consist of the upper rebar with a diameter of 13 mm, the lower rebar with a diameter of 8 mm, the lattice steel wire with a diameter of 5.0 mm, and the deck plate with a thickness of 0.5 mm. The test and measured construction loads for evaluation of deflection were virtually the same as 4.70 kN/m².

The distributed loads as a function of deflection for the two specimens are shown in Figure 12. The maximum deflections at the center of 150-ED3-3.8A and B for the specified construction load

were measured as 27.3 mm and 24.4 mm and the residual deflections were 0.52 mm and 0.01 mm at the unloading with the restoration rate of 98.1% and 99.9%, respectively. Similar to specimens 135-ED1-3.2A and B, the left and right deflections with increasing loads were quite similar.

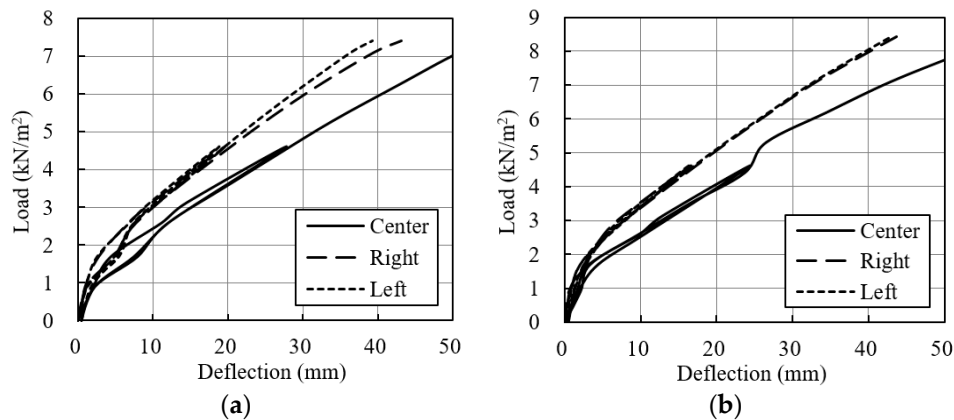


Figure 12. Distributed load as a function of deflection for (a) Specimen 150-ED3-3.8A and (b) Specimen 150-ED3-3.8B.

4.4. Specimens 200-ED5-4.5A and B

Specimens 200-ED5-4.5A and B were prepared to have the depth of 200 mm and the span length of 4.5 m and consist of the upper rebar with a diameter of 13 mm, the lower rebar with a diameter of 13 mm, the lattice steel wire with a diameter of 6 mm, and the deck plate with a thickness of 0.5 mm. These specimens were evaluated for the measured construction load of 5.85 kN/m², which was almost the same as the specified value of 5.90 kN/m².

Figure 13 shows the test results of distributed loads as a function of deflection. The deflections for specimen 200-ED5-4.5A and B were measured as 26.1 mm and 22.4 mm, respectively; the residual deflections were 0.07 mm for specimen A with a restoration rate of 99.7% and 0.23 mm for specimen B with a recovery rate of 99.0%. The left and right deflections were also similar for both specimens.

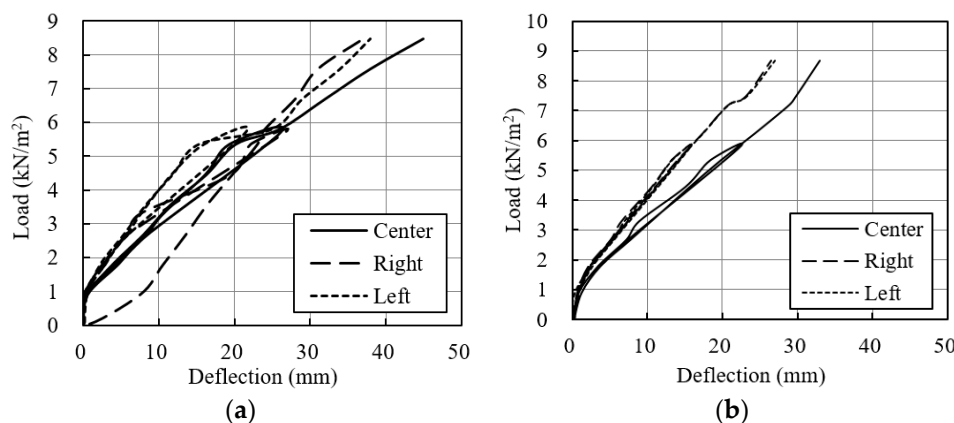


Figure 13. Distributed load as a function of deflection for (a) Specimen 200-ED5-4.5A and (b) Specimen 200-ED5-4.5B.

4.5. Local Responses

Local responses of test specimens with a focus on the failure modes were examined using the test data measured from strain-gauges. Figure 14 shows distributed load as a function of strain measured for 135-ED1-3.2A and B. The maximum strains for both specimens A and B occurred at the center of upper rebar and were around 0.0015, and both failed for the maximum load of 6.84 kN/m² due to the

elastic buckling of the upper rebar on center in the tests, noting that the yield strain of the upper rebar with a diameter of 10 mm was 0.00270, as shown in Table 3.

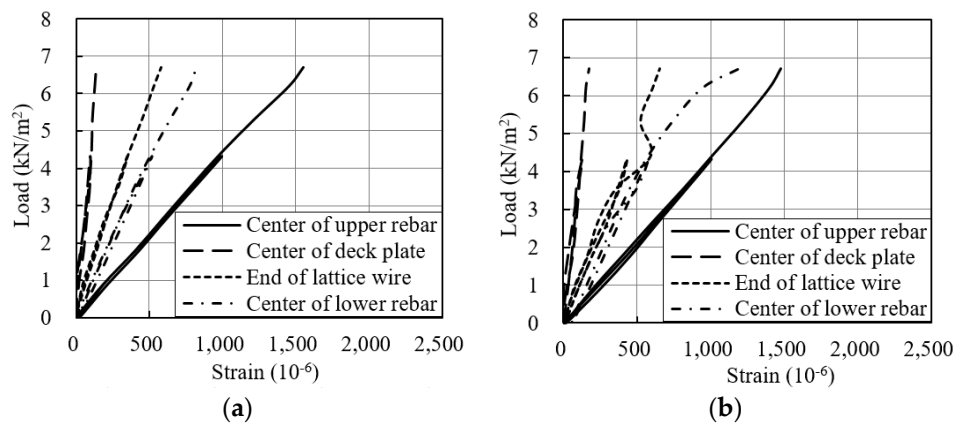


Figure 14. Distributed load as a function of strain for (a) Specimen 135-ED1-3.2A and (b) Specimen 135-ED1-3.2B.

Applied loads as a function of strain for specimens of 150-ED3-3.8A and B are shown in Figure 15. A compression failure from the lattice steel wire near the end was observed for 150-ED3-3.8A when the maximum load of 7.57 kN/m² was reached, although the maximum strains occurred on the center of the lower rebar. A different failure mode was observed for 150-ED3-3.8B, where this specimen failed at the maximum load of 8.59 kN/m² due to the buckling of the upper center rebar. Different failure modes were generated for specimens A and B, but this have insignificant influence on the global deflections of the test specimen. The maximum strain was measured as 0.00216 at the center of upper rebar of 150-ED3-3.8B, but it did not exceed the yield strain of 0.00233, indicating all measured strains for 150-ED3-3.8A and B were within the elastic range.

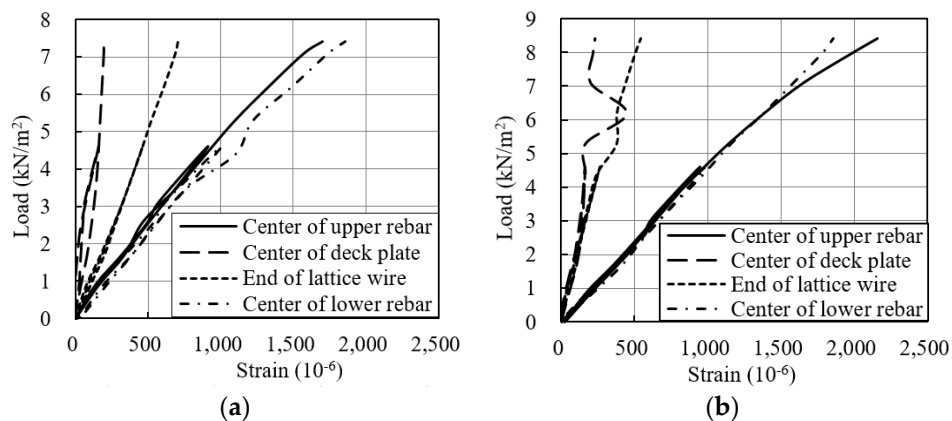


Figure 15. Distributed load as a function of strain for (a) Specimen 150-ED3-3.8A and (b) Specimen 150-ED3-3.8B.

Similar to the 135 and 150 specimens, the maximum strains for both 200-ED5-4.5A and B occurred at the center of upper rebar. However, the measured values of approximately 0.0010 for both, as identified in Figure 16, were somewhat smaller than those of others specimens, which can be attributed to welding failure modes at joints connecting the lower rebar and the lattice steel wire. Although this welding failure occurred after the specified construction load was reached, it might be necessary to propose a method to secure the welding strength between the lower rebar and the lattice wire, thereby improving the strength of the 200-ED5-4.5 specimens.

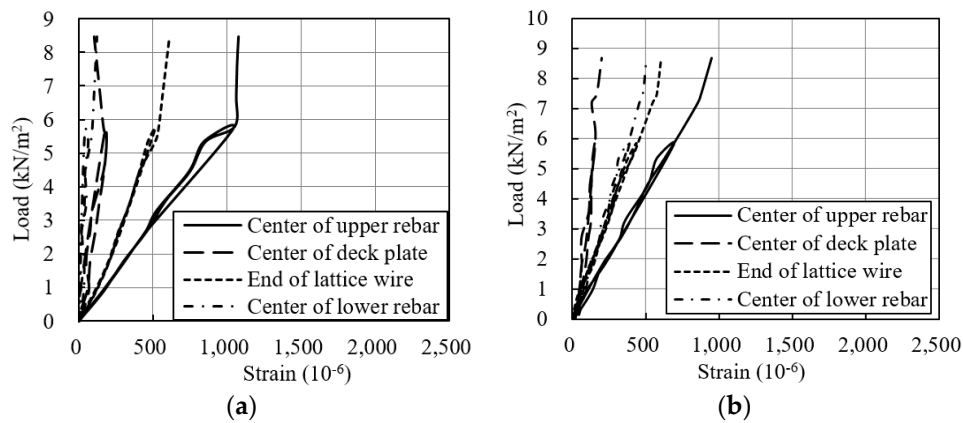


Figure 16. Distributed load as a function of strain for (a) Specimen 200-ED5-4.5A and (b) Specimen 200-ED5-4.5B.

4.6. Test-Result Summary

Test results conducted for six specimens of truss girder-bolted deck plate are summarized in Table 4 and Figure 17. All specimens lead to the maximum measured deflections less than the design deflections for the specified construction loads, as shown clearly in Figure 17a, and the restoration rates greater than 97%, as shown in Figure 17b. The measured deflection for 150-ED3-3.8A exceeded 95% of the design value, but when taking into account the restoration rate of 98.1%, the structural resistance of the specimen to the specified construction load is considered to be sufficient because all members of this specimen are considered to exhibit nearly elastic behavior. It is also noted that the loading conditions used in the tests were conservative than in the field, that is, all loads in the tests were applied to the deck plate, but on a construction site, the workload is applied practically to the upper rebar and the self-weight of the concrete is applied to the deck plate.

Table 4. Test results.

Specimen ID	Construction Load (kN/m ²)		Measured Deflection (mm)	Design Deflection (mm)	Measured/Design (%)	Residual Deflection (mm)	Restoration Rate (%)	Max Load (kN/m ²)
	Planned	Measured						
135-ED1-3.2A	4.35	4.38	20.5	25.5	80	0.57	97.2	6.84
135-ED1-3.2B	4.35	4.38	23.0	25.5	90	0.40	98.3	6.84
150-ED3-3.8A	4.70	4.70	27.3	28.5	96	0.52	98.1	7.57
150-ED3-3.8B	4.70	4.70	24.4	28.5	86	0.01	99.9	8.59
200-ED5-4.5A	5.85	5.90	26.1	32.0	82	0.07	99.7	8.64
200-ED5-4.5A	5.85	5.90	22.4	32.0	70	0.23	99.0	8.86

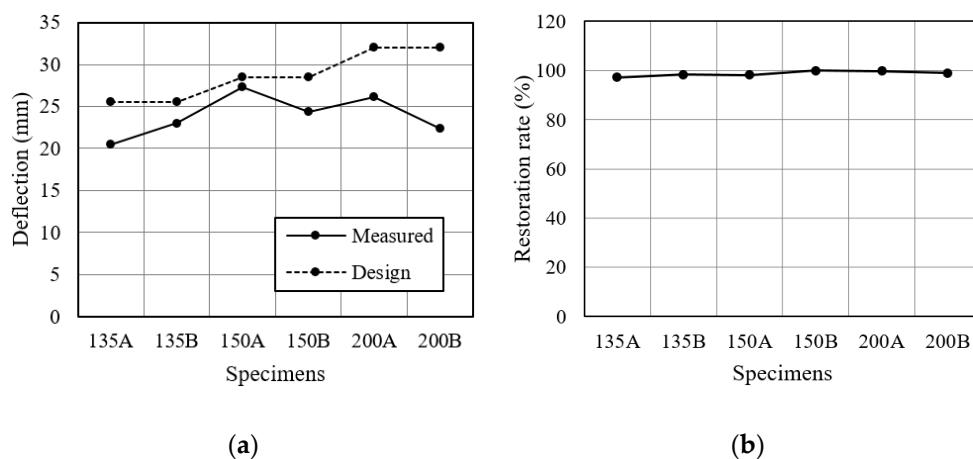


Figure 17. Deflections and restoration rate varying specimen. (a) Deflection. (b) Restoration rate.

5. Numerical Investigation

5.1. Finite Element Modeling

The deck plate bolted with truss girder has been numerically modeled based on the test results to further examine the structural responses not identified from the tests. A finite element code, LS-DYNA [14,15], was employed for these simulations. The deck plate was modeled using shell elements with the Belytschko–Tsay element formulation with two through thickness integration points. The truss girder consisting of upper rebar, lower rebar, and lattice steel wire was modeled using the Hughes–Liu element formulation with the cross-section integration with the 2×2 Gauss quadrature rule. The spacers, which enable connection of deck plates and truss girders by bolts, were modeled using one-point quadrature eight-node solid elements, with which the Flanagan–Belytschko hourglass control with exact volume integration for solid elements and the hourglass coefficient of 0.1 recommended by Erhart [21] was defined using CONTROL_HOURLASS to prevent the zero energy deformation modes.

A full-scale model for each specimen has been built, as shown in Figure 18a for 135-ED1-3.2. All steel components were connected by merging nodes assuming perfect bond. The models were simply supported at 50 mm away from the ends, similar to the given experimental conditions. An element size of approximately 8 mm was used consistently for beam, shell, and solid elements and this size has been considered to be sufficient to result in mesh-converged solutions. Figure 18b shows the modeling details including the information for element size in the vicinity of the support. The global and local responses of the numerical models are evaluated later in this paper by comparison to the test results.

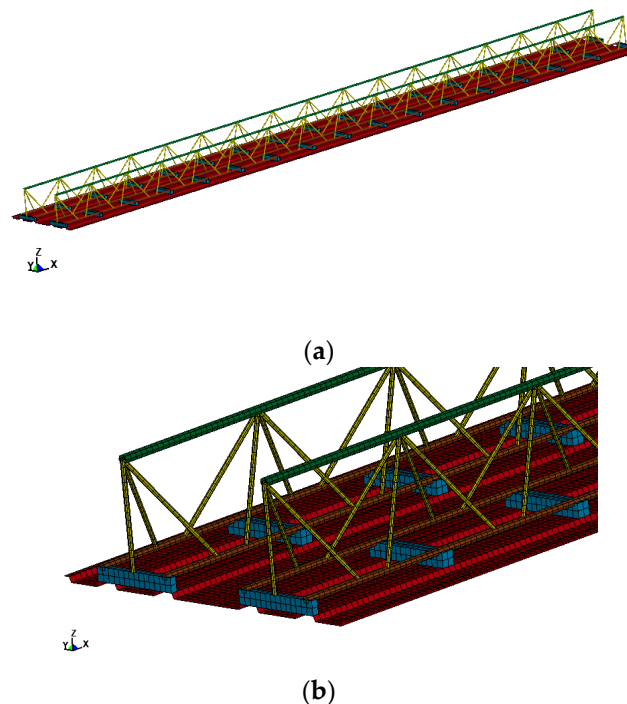


Figure 18. Numerical model for Specimen 135-ED1-3.2. (a) Full-scale numerical model. (b) Mesh in the vicinity of the support.

5.2. Material Model

Deck plates, truss girders including upper rebar, lower rebar, and lattice wire and spacers were modeled consistently using MAT_PLASTIC_KINEMATIC, which was defined with a perfectly elastic–plastic material to reduce the numerical difficulty and to improve the computational efficiency,

noting that the test specimens were intended to maintain the elastic state. The stress–strain relationships were defined on the basis of the material test data with no tangent modulus assuming the perfectly elastic–plastic behavior.

5.3. Simulation Results

Numerical results for the truss girder-bolted deck plates are evaluated based on the test results described previously. Table 5 and Figure 19 enable a comparison of deflection between numerical calculations and test results with respect to the specified construction loads. The numerically-computed deflection for both 135-ED1-3.2A and B is 22.5 mm, which is fairly similar to the two measured deflections, as shown in Table 5. This is similar for other numerical results. Moreover, all measured and numerical deflections are smaller than the design deflections defined previously.

Table 5. Comparison of deflection between numerical predictions and test results.

Specimen ID	Measured Construction Load (kN/m ²)	Measured Deflection (mm)	Numerical Deflection (mm)	Design Deflection (mm)
135-T1-3.2A	4.38	20.5	22.5	25.5
135-T1-3.2B	4.38	23.0	22.5	25.5
150-T3-3.8A	4.70	27.3	23.0	28.5
150-T3-3.8B	4.70	24.4	23.0	28.5
200-T5-4.5A	5.90	26.1	22.0	32.0
200-T5-4.5A	5.90	22.4	22.0	32.0

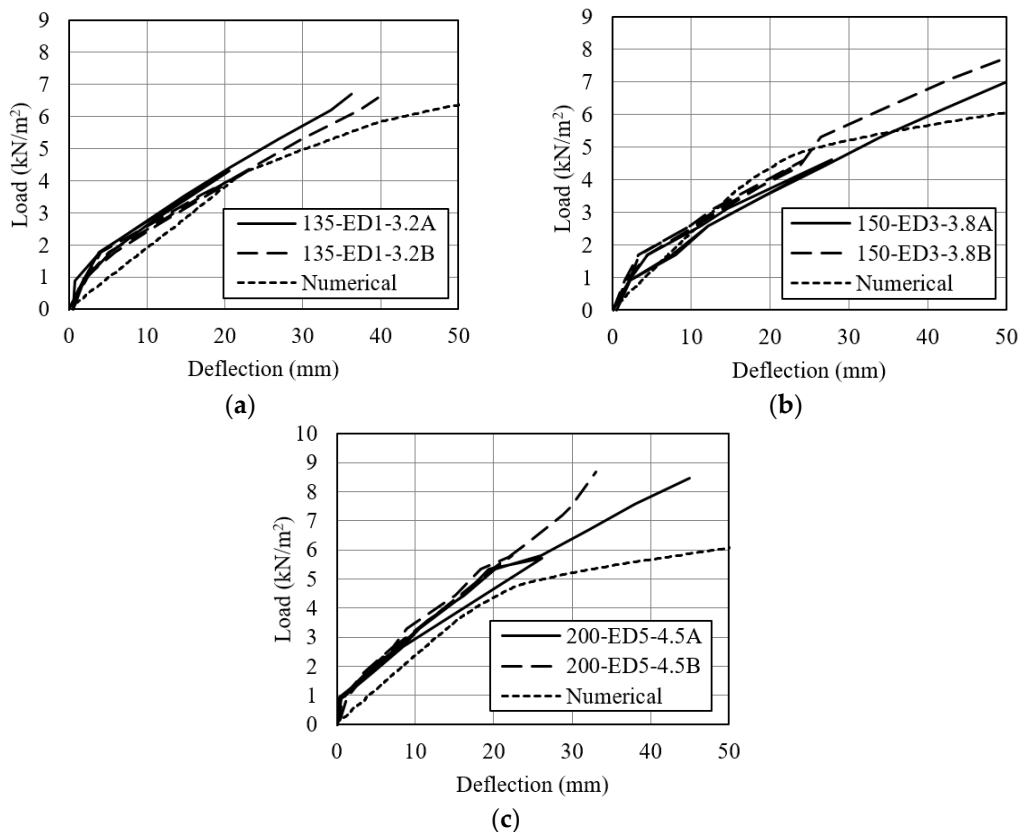


Figure 19. Distributed loads as a function of deflection between numerical predictions and test results. (a) Specimen 135-ED1-3.2. (b) Specimen 150-ED3-3.8. (c) Specimen 200-ED5-4.5.

Figure 19 shows distributed loads as a function of deflection for the three types of numerical model. It is seen that all numerical models lead to the deflections varying the distributed load,

reasonably similar to the test results. Some differences are, however, observed in the initial slopes for most specimens, that is, the initial slopes tend to be greater than those for numerical models. This is because the specimens were somewhat unstable in the early stage of the tests, noting that the specimens were simply supported without any constraints at both ends. The slopes stabilize after a particular level of load is reached. After the specified construction loads are reached, the numerically-calculated deflections, especially for 200-ED5-4.5, tend to diverge from the measured deflections, which is attributed to the perfectly elastic–plastic behavior defined for all steel members. Nonetheless, this difference is insignificant in this study because the range of interest in the numerical simulations is the region below the specified construction load, and within this range, the results are sufficiently comparable.

Figure 20 shows distributions of von Mises stress and axial stress generated from numerical simulations for deck plate and truss girder of 135-ED1-3.2 for the construction load of 4.38 kN/m^2 used for evaluation of deflection. It is observed that stresses for both deck plate and truss girder are localized near the supports. This stress localization along with the failure modes of test specimens is discussed in detail later in this paper.

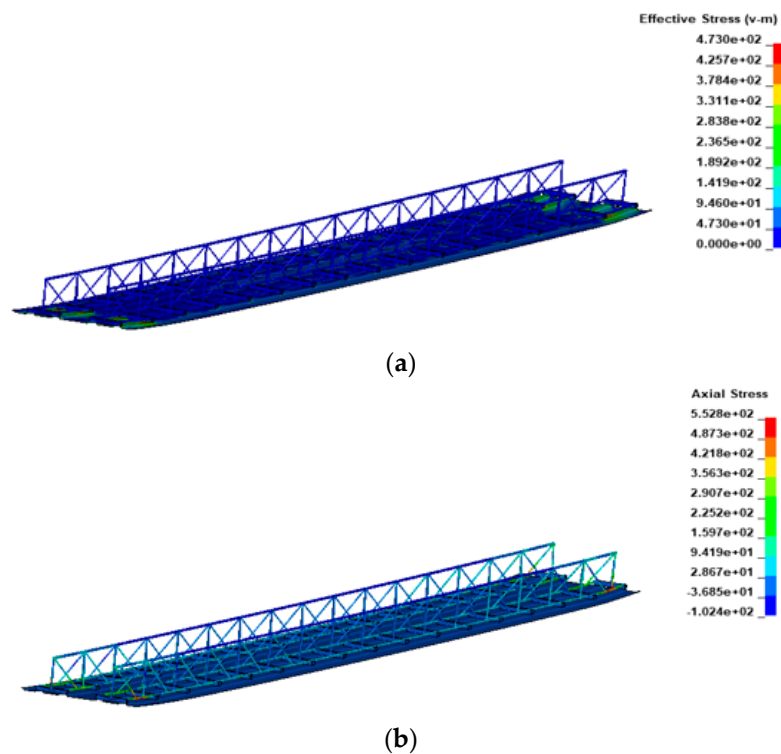


Figure 20. Simulation results for Specimen 135-ED1-3.2. (a) von Mises stress distribution for deck plate. (b) Axial stress distribution for truss girder.

5.4. Failure Mode

Table 6 enables a comparison of failure mode between numerical predictions and test results. Similar failure modes occurred for all three numerical models: buckling of the lower rebar and lattice steel wire near the end of the models. However, the test specimens of 135-ED1-3.2A and B and 150-ED3-3.8B led to quite different failure modes from the numerical models, where these specimens failed due to the buckling of the upper truss near the center of the specimen. This may be attributed to the step-by-step loading method from the center to the end, described previously, in the tests, which indicates that the deck plate with truss girder can fail near the end rather than the center in practice. On the other hand, the specimen 150-ED3-3.8A failed by buckling of lattice near the end, similar to the corresponding numerical model. Also, the welding failures for the specimens of 200-ED5-4.5A and B

can be regarded as reasonably comparable to the numerical results because the failure locations are similar and these failures can occur due to the buckling and the stress concentration observed in the numerical results.

Table 6. Failure modes between numerical models and test specimens.

Specimen ID	Test Specimens	Numerical Models
135-ED1-3.2A 135-ED1-3.2B	Buckling of upper truss near the center Buckling of upper truss near the center	Buckling of lower truss and lattice near the end
150-ED3-3.8A 150-ED3-3.8B	Buckling of lattice steel wire near the end Buckling of upper truss near the center	Buckling of lower truss and lattice near the end
200-ED5-4.5A 200-ED5-4.5A	Welding failure at joints between the bottom rebar and lattice steel wire Welding failure at joints between the bottom rebar and lattice steel wire	Buckling of lower truss and lattice near the end

The buckling for each numerical model is also identified in the numerically-calculated von Mises stresses as a function of distributed load, shown in Figure 21. It is evident that the von Mises stresses abruptly decreases due to the buckling when particular loads are reached, noting that the buckling loads are identified quite after the specified construction loads. An observation is also made that the stresses are less localized on the center of upper rebar than other components. Figure 22 shows contours of von Mises stresses and effective plastic strains for 135-ED1-3.2 and is provided to clearly give the specific failure locations, which is situated near but somewhat away from the end.

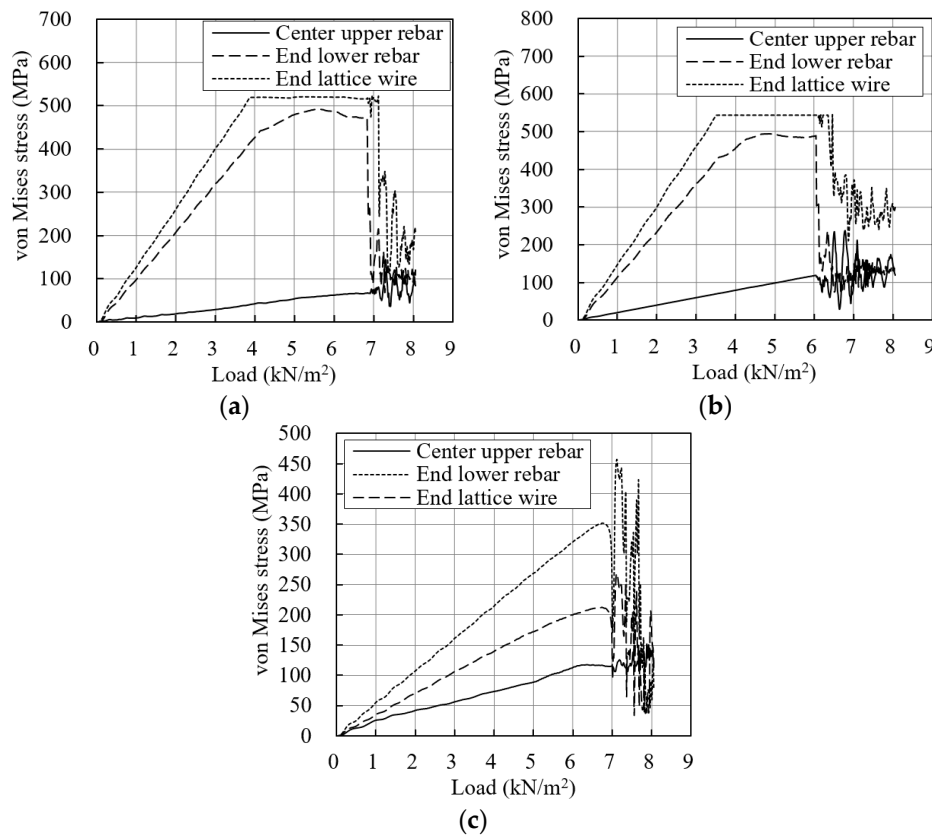


Figure 21. von Mises stresses as a function of distributed load for numerical models. (a) Specimen 135-ED1-3.2. (b) Specimen 150-ED3-3.5. (c) Specimen 200-ED5-4.5.

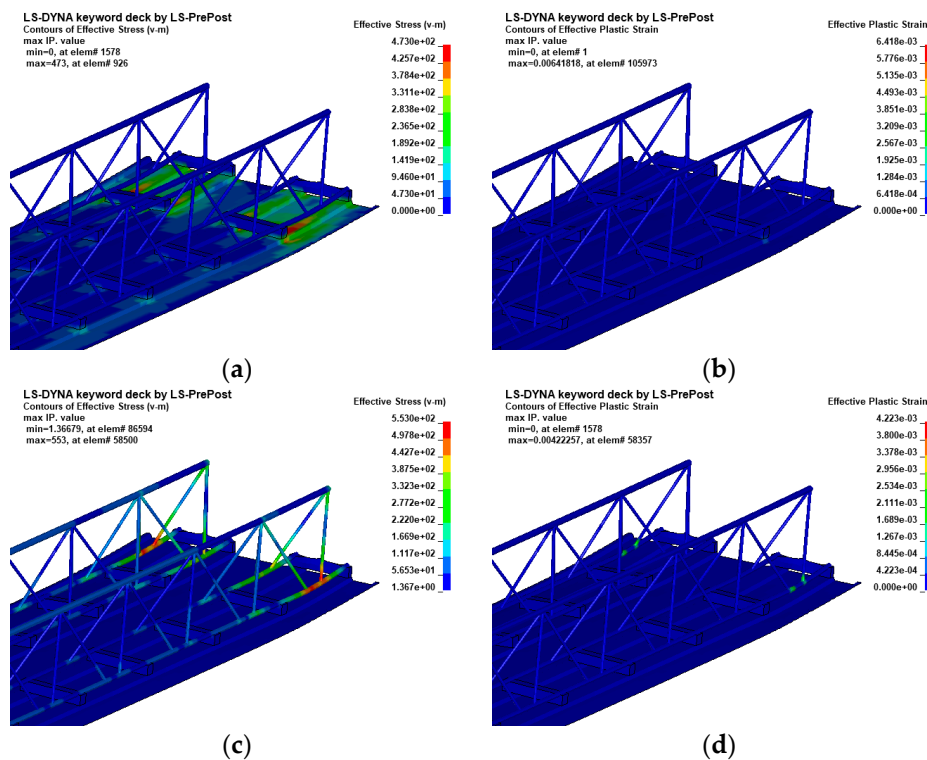


Figure 22. von Mises stresses and effective plastic strain for deck plate and truss girder in the vicinity of the support for 135-ED1-3.2. (a) von Mises stress for deck plate. (b) Effective plastic strain for deck plate. (c) von Mises stress for truss girder. (d) Effective plastic strain for truss girder.

6. Conclusions

This study presents an experimental and numerical study for evaluation of the structural safety of a deck plate bolted with truss girder. This deck-plate system has been proposed to resolve the welding issues. In total, six tests on a full scale were performed to examine the structural performance of the proposed system. The test specimens were evaluated for the specified construction loads based on the deflection criteria provided in AIK [16], which is more conservative than those of ASCE [17]. The local responses of the specimens were investigated using the strain-gauge measurements. Numerical simulations for all test specimens were then conducted to ensure that the test results are reliable and to further investigate the responses, which could not be clearly accounted for in the tests. The key findings and recommendations are as follows:

1. The structural safety of the proposed truss girder-bolted deck-plate system has been validated through experimental and numerical studies. All test specimens and the relevant numerical models met the provided design deflection criteria for given construction loads.
2. The restoration capability has been experimentally validated. Most members of the test specimens remain nearly elastic, noting that the restoration rates were greater than 97% for all specimens.
3. The numerically-predicted deflections were very similar to the measured values until the specified loads is reached, ensuring the reliability of the test results. Some differences were observed after the specified loads due to the use of the elastic–plastic material models, but this is insignificant because the evaluation of the deflection is aimed at the specified loads.
4. A few test specimens failed due to the buckling of the center upper rebar, but the relevant numerical results indicate that the specimens can show different failure modes of the buckling of the lower rebar and the lattice steel wire near the end, noting that the test specimens were loaded using the step-by-step loading method conservatively from the center to the ends.

5. The test results showed that the welding issues between the deck plate and truss girder can be resolved with the bolted system, but other welding problems in the region of joints between the lower rebar and lattice steel wire can be posed, even though the welding failures occurred after the specified loads. Stress localization was also observed in the numerical simulations in the locations of the welding failures in the tests, which indicates that the details in these areas need to be modified to improve the structural performance of the proposed deck-plate system.

Author Contributions: The authors contribute as follows: Conceptualization, J.S., J.L., and B.K.; data curation, Y.L.; Formal analysis, J.S. and J.L.; funding acquisition, J.S.; investigation, J.S. and B.K.; methodology, Y.L. and B.K.; project administration, B.K.; resources, J.L.; software, J.S.; validation, J.S. and B.K.; visualization, J.S. and J.L.; writing—original draft, J.S.; writing—review and editing, Y.L. and B.K.

Funding: This work was supported by the National Research Foundation of Korea (NRF) grant funded by the Korean Government (MSIT) (No. NRF-2018R1C1B6006275).

Conflicts of Interest: The authors declare that they have no conflicts of interest.

References

1. Moon, T.S.; Bae, J.W. An analytical study on the structural behavior of the composite slab with new-shaped deckplate. *J. Korean Soc. Steel Constr.* **1999**, *11*, 181–190.
2. Choi, S.-M.; Tateishi, K.; Uchida, D.; Asano, K.; Kobayashi, K. Fatigue strength of angle shape shear connector used in steel-concrete composite slab. *Int. J. Steel Struct.* **2008**, *8*, 199–204.
3. Kim, Y.-J.; Oh, S.-H.; Yoon, M.-H.; Lee, Y.-H.; Kim, H.; Byon, E. Experimental investigation of deck plate system with non-welding truss type deformed steel wires (TOX deck plate slab). *Int. J. Steel Struct.* **2009**, *9*, 315–327. [[CrossRef](#)]
4. Ko, T.-H.; Yoon, J.-H.; Seo, D.-W.; Chang, K.-K. Structural behavior evaluation of deck plate slab with inverted triangle truss type bar. In Proceedings of the Annual Conference of the Architectural Institute of Korea, Seoul, Korea, 23 October 2010.
5. Kang, M.-J.; Kim, S.-S. Structural Performance Evaluation of Steel Wire-Integrated Deck Plate according to the Construction Load. *J. Archit. Inst. Korea* **2015**, *31*, 3–12.
6. Oh, S.H.; Kim, Y.J.; Yoon, M.H. Test on the structural performance of the TOX deck plate-evaluation of structural safety during construction stage. *J. Korean Soc. Steel Constr.* **2008**, *20*, 701–709.
7. Kim, Y.-J.; Chai, H.-S.; Kim, W.-J. A study of the experimental for the shear bond strength of deck plate composite slabs. *J. Archit. Inst. Korea* **2005**, *25*, 237–240.
8. Lee, S.-K.; Lee, Y.-J. An evaluation of structural safety for steel wire-integrated deck plate system. *J. Archit. Inst. Korea* **2007**, *23*, 43–50.
9. Lee, Y.-J.; Yoon, S.-C. Development of steel wire-integrated deck plate applicable to slab with 180 mm thickness. *J. Korean Inst. Struct. Maint. Insp.* **2012**, *16*, 89–98.
10. Kim, S.-B.; Kang, M.-J.; Hwang, B.-C.; Kim, S.-S. Structural performance evaluation for steel wire-integrated deck plate according to the diameter of the lattice bar. *J. Korean Soc. Hazard Miti.* **2014**, *14*, 1–9.
11. Lee, K.-J.; Kim, W.-Y.; Jung, J.-W.; Kim, E.-K.; Yang, I.-S. Structural performance of RC slab using steel wire integrated deck plate. In Proceedings of the Annual Conference of the Architectural Institute of Korea, Seoul, Korea, 21–23 June 2014.
12. Lee, Y.-J.; Yi, W.-H. The study of corrosion for steel wire-integrated deck plate. *J. Archit. Inst. Korea* **2009**, *25*, 137–144.
13. Jung, H.-S.; Choi, C.-S.; Choi, Y.-S. A study on the improvement of construction performance for removable form deck plate method. In Proceedings of the Korea Concrete Institute 2017 Fall Conference, Seoul, Korea, 1–3 January 2017.
14. LSTC. *LS-DYNA Keyword User's Manual*; Livermore Software Technology Corporation: Livermore, CA, USA, 2018.
15. LSTC. *LS-DYNA Theory Manual*; Livermore Software Technology Corporation: Livermore, CA, USA, 2006.
16. AIK. *Standard and Commentary for Composite Metal Deck Slab System Design*; Architectural Institute of Korea: Seoul, Korea, 1998.
17. ASCE. *Standard for the Structural Design-Composite Slabs, ANSI-ASCE3-91*; ASCE: Reston, VA, USA, 1992.

18. KATS. *Low Carbon Steel Wires, KS D 3552*; Korean Agency for Technology and Standards: Eumseong-gun, Korea, 2014.
19. KATS. *Hot-Dip Zinc-Coated Steel Sheets and Coils, KS D 3506*; Korean Agency for Technology and Standards: Eumseong-gun, Korea, 2016.
20. Lee, J.-E. Performance Evaluation of Bolt Joint Type Removable Truss Deck Plate for Field Application. Ph.D. Thesis, Department of Architectural Engineering, Catholic Kwandong University, Gangneung, Korea, 2015.
21. Erhart, T. Review of solid element formulations in LS-DYNA, LS-DYNA. In Proceedings of the LS-DYNA Developers' Forum, Stuttgart, Germany, 12 October 2011.



© 2019 by the authors. Licensee MDPI, Basel, Switzerland. This article is an open access article distributed under the terms and conditions of the Creative Commons Attribution (CC BY) license (<http://creativecommons.org/licenses/by/4.0/>).